# On Flare Productivity of Active Regions

A thesis submitted towards partial fulfilment of
BS-MS Dual Degree Programme

by

Revati Sudam Mandage

under the guidance of

Dr. R. T. James McAteer

New Mexico State University

Indian Institute of Science Education and Research
Pune

# Certificate

This is to certify that this thesis entitled "On Flare Productivity of Active Regions" submitted towards the partial fulfilment of the BS-MS dual degree programme at the Indian Institute of Science Education and Research Pune represents original research carried out by "Revati Sudam Mandage" at "New Mexico State University", under the supervision of "Dr. R. T. James McAteer" during the academic year 2014-2015.

Student
REVATI
MANDAGE

Supervisor
DR. R. T. JAMES
MCATEER

# Declaration

I hereby declare that the matter embodied in the report entitled On Flare Productivity of Active Regions are the results of the investigations carried out by me at the Department of Astronomy, New Mexico State University, under the supervision of Dr. R. T. James McAteer and the same has not been submitted elsewhere for any other degree.

Student
REVATI SUDAM
MANDAGE

Supervisor
DR. R. T. JAMES
MCATEER

# Acknowledgements

I am thankful to Indian Institute of Science Education and Research(IISER), Pune and New Mexico State University (NMSU) for giving me the opportunity to carry out this research work at the Department of Astronomy, NMSU.

I am much grateful to my advisor, Dr. R. T. James McAteer, for his guidance, encouragement and for making this research work a wonderful learning experience.

Finally, I would like to thank my parents and my friends for their help and support.

# Abstract

Magnetic power spectral analysis was performed on HMI/SDO magnetograms to see the relationship between power index values and flare productivity of active regions.

Out of 52 HMI active region patches (HARP), observed during August 2011 to July 2012, 24 HARPs showed no flare activity at all, 19 HARPs were moderately flare active with at least one flare of the intensity between M1 to M5 whereas 9 HARPs showed high flare activity with at least one flare of the intensity greater than M5.

Power index was computed for these regions as they travelled across the solar disk. We found that regions that showed extreme flare activity tend to have high power index ($\sim 2.2$) whereas regions that showed no flare activity are likely to have low power index values ($\sim 1.6$) but may take higher power index values indicating high power index is not a sufficient condition for flaring.

# Contents

# Chapter 1

# Introduction

Solar events such as solar flares and coronal mass ejections (CME) are observed in the solar atmosphere. Magnetic fields, present in the solar photosphere, interact with plasma flows. When the magnetic Reynolds number is high these plasma flows happen to be in a state of turbulence.

Magnetic fields are present in the form of thin vertical flux tubes. Motion of these flux tubes is governed by turbulent plasma flows. Turbulence state of plasma determines concentration of the flux tubes, diffusion of flux tubes as well as the energy dissipation of the system.

## 1.1 Active Regions

Active regions are the regions in the photosphere where intense magnetic fields are present. Active regions happen to be very dynamic in the sense that magnetic flux tubes in these regions can get concentrated or decayed or rearranged.

Active regions are also the regions of high solar activity. Activity of a region can be decided in terms of flare productivity of that region. Some active regions tend to produce very powerful and numerous solar flares whereas some regions produce less intense and less numerous flares. This flare productivity may depend on how turbulent a region is. Studying power spectrum is one way to understand the state of turbulence of an active region.

## 1.2 Power Spectrum

Power spectrum gives information about the amount of power contained in structures at different length scales. Injection of energy into large scaled structures, energy dissipation at small scaled structures and the transfer of energy across the intermediate structures are represented in the power spectrum. Structure of a power spectrum tells us about the energy transfer mechanisms e.g. presence of inverse cascade represent the formation of large scaled structures from small scaled structures. This spectrum is obtained in the frequency domain.

Power spectrum consists of three sub-ranges: Injection range, inertial range and dissipation range. Injection range occurs at low wavenumbers. This is the range where energy is injected into the system. Inertial range occurs at intermediate wave numbers. In this range, power cascades down at a constant rate from large to small structures (low to high wave numbers). For this range, power spectrum takes the form of $E(k) \sim k^{-\alpha}$. This expression is called power law where $\alpha$ is known as power index which describes the rate of power transfer in the inertial range [7]. At high wave numbers dissipation range is observed where energy dissipates into the heat.

In the absence of magnetic fields, kinetic energy spectrum can be described by Kolmogorov spectrum, $\alpha{\sim}5/3$ [5]. but in the presence of magnetic fields, the spectrum may take a form of $\alpha{\sim}3/2$ [4, 6].

Power law index values help us see the nature of the turbulence of an active region. Kolmogorov type spectra indicate homogeneous stationary MHD turbulence wherein a dynamic equilibrium exists between input of energy at large scale and the output of energy at small scales. Non-Kolmogorov type steep spectra shows the presence of inhomogeneous non-stationary MHD turbulence. in such cases system may go through catastrophes.

Studies of calculating magnetic power spectra have been done in the past but studies on relating magnetic spectral analysis with flare activity of regions are rare.[2].In such studies of calculating magnetic power spectra, MDI/SOHO line-of-sight magnetograms with a resolution of 1.98 arc-sec per pixel length have been used. These magnetograms provide line of sight information of magnetic fields. Spectral analysis performed on 16 active regions by Abramenko [2] demonstates that higher flare productivity is related with steeper magnetic power spectrum and regions that produced X-class flares possessed a steep power spectrum with $\alpha > 2.0$. In the present work we analyse HMI/SDO (Helioseismic Magnetic Imager) vector magnetograms with a resolution of 0.5 arc-sec per pixel length of 52 HARPs (HMI active region patches) in order to see the relationship between the power index values and flare activity of these regions.

# Chapter 2

# Data

Magnetograms are images of active regions on the sun that provide magnetic field information of these regions. For this study we used HMI/SDO magnetograms. These magnetograms are vector magnetograms and hence they provide magnetic field information in all three components viz., r, $\theta$ and $\phi$.

Our data includes HMI/SDO vector magnetograms of 52 HMI active region patches (HARP) observed during August 2011 to July 2012.

These HARPs were categorized as per the intensities of the flares they produced. Active regions that produced at least one flare whose intensity was greater than M5 were considered to be highly flare productive regions while regions that gave out at least one flare with intensity more than M1 but less than M5 were considered to be moderately flare productive regions. Active regions that did not produce any flare of intensity greater than C1 were considered to be flare-quiet active regions. Out of 52 HARPS, 24 HARPs showed no flare activity at all, 19 HARPs were moderately flare productive with at least one flare of intensity between M1 to M5 whereas 9 HARPs showed extremely high flare productivity with at least one flare of intensity greater than M5.

6-7 images per day with a cadence of one hour per HARP were analysed as it travelled across the solar disk. Resolution for each image is 0.5 arc-sec per pixel length. Since HMI/SDO magnetograms provide magnetic field information in all three components, vector magnitude is considered for magnetic power spectral calculations.

# Chapter 3

# Methods

In order to obtain power index values for the active regions, we need to obtain the power spectrum. Power spectrum is obtained using Fourier Transform. Once the power spectrum is obtained a proper inertial range is chosen in order to compute the slope or in other words, the power index.

It is necessary to carefully crop images in order to exclude low-value quiet sun portion around the sun-spots. Since it lowers down the average energy while computing the power spectrum, it may affect the slope calculations.

## 3.1 Magnetic Power Spectrum

The Energy Spectrum of 2D function is obtained as [7]:

$$F(\mathbf{k}) = |U(\mathbf{k})|^2$$

Here $U(\mathbf{k})$ is the Fourier transform of an image $U(\mathbf{I})$ and $\mathbf{k}$ is the wave vector.

To compute the magnetic power spectrum we used the technique described in [1] :

Define a rectangular grid $\omega$ to specify $U(\mathbf{I})$ as follows:

$$\omega : (x_i = i, i = 1, ...., N_x; y_j = j, j = 1, ...., N_y)$$

Define another rectangular grid $\Omega$ to specify $U(\mathbf{k})$ which are complex numbers:

$$\Omega : (k_{x,i} = i\Delta k_x, i = -(N_x/2-1), ...., N_x/2; k_{y,j} = j\Delta k_y, j = -(N_y/2-1), ...., N_y/2)$$

here $\Delta k_x = 2\pi/(N_x \Delta x)$ and $\Delta k_y = 2\pi/(N_y \Delta y)$.

In order to calculate power spectrum, $F(\mathbf{k})$ needs to be shifted in such a way that the zero frequency is at the center of the co-ordinate system. Power spectrum is defined as [7] :

$$E(k) = \int\limits_{|\mathbf{k}|=k} F(\mathbf{k})\, dS(\mathbf{k})$$

Here $k = \sqrt{k_x^2 + k_y^2}$ with $k_x$ and $k_y$ are the spatial frequency values along the respective axes and $dS(\mathbf{k})$ is a length element of circle with radius $k$. To calculate the power spectrum, mean value theorem can be applied to above integral:

$$E(k_m) = dS(|\mathbf{k}| = k) \sum_{k_m-(dk/2)\leq|\mathbf{k}|_m+(dk/2)} F(k_x, k_y)/N(k_m)$$

here $N(k_m)$ are the points inside an annulus bounded by two circles of radii $k_m - dk/2$ and $k_m + dk/2$. Length of the element of circle $|\mathbf{k}| = k$ should be chosen carefully since the area is bounded by the maximum and minimum frequency values. The width of the annulus is defined as follows:

$$dk = p\sqrt{\Delta k_x{}^2 + \Delta k_y{}^2}$$

Here $p$ is a real number. $p$ is chosen in such a way that the spectrum will be properly resolved, without much affecting the slope. In order to get optimum spacing, slope is calculated at different $p$ values (from 1 to 1.5). Since the slope values don't change much, $p$ corresponding to a slope value which is close to the averaged slope value is considered to be an optimum multiplier.

## 3.2 Image Correction

HMI/SDO magnetograms include magnetic field information about active region groups (NOAA) as well as about the quiet sun region around them. Magnetic field values for this region tend to be less trustworthy and hence while computing the power spectrum it lowers down the average, slightly distorting the spectrum. and this may affect the power index calculations.

In order to exclude the quiet sun data carefully following method is adopted: Magnetic field values are added along columns and normalized (xvalues) (fig 3.2 a) and along rows and normalized (yvalues) (fig 3.2 b). These values are normalized so that the method can be applied to all the images. Since the vector magnitude is considered, these values are positive. The image is cropped in x direction, keeping number of pixels in y direction

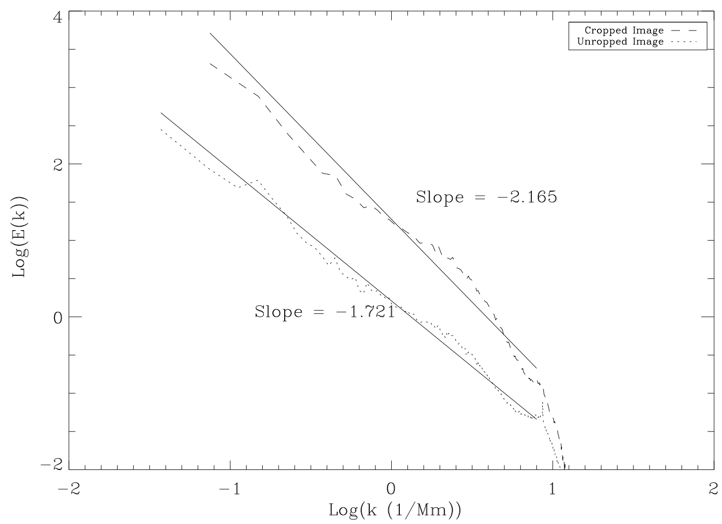


Figure 3.1: Dotted line indicates the spectrum for original mangetogram of HARP 1028. Dashed line shows the spectrum for the carefully cropped magnetogram .

constant, at 10 different steps in such a way that the first and last pixels are the points where xvalues are greater than chosen limits, from 0.0 to 0.9. Power spectrum is obtained and the slope is calculated at every step (fig. 3.2 c) The image is cropped in a same way in y direction, keeping number of pixel in x direction constant, at 10 different steps. The first and the last pixels are the points where yvalues are greater than chosen limits, from 0.0 to 0.9. Slope is calculated at every step. (fig. 3.2 d)

Values of the slope, in both cases, drops down considerably when most of the quiet sun portion is excluded. After a certain step slope does not change much with cropping. This step is considered to obtain the first and last pixels in x and y direction to crop the image.

## 3.3 Inertial Range

Inertial range of the power spectrum can be identified using the spectral discontinuities. The first spectral discontinuity occurs at the wave number where the energy is maximum. It separates injection range from the inertial range. The second spectral discontinuity separates inertial range from dissipation range.

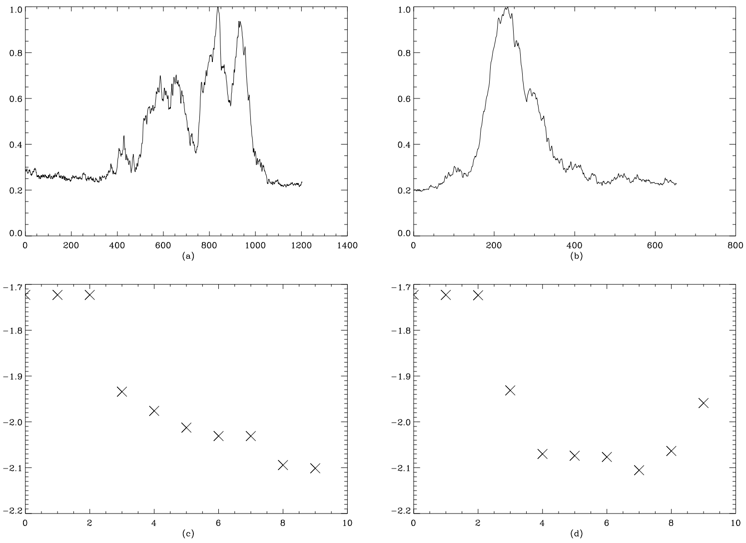


Figure 3.2: Fig. c and fig. d show slope values for the image of HARP 1028 cropped at different steps. First three slope values are same since all xvalues and yvalues are above 0.2. When the image is cropped considering the points where xvalues and yvalues are above 0.3, we see a sharp deep in the slope. This happens due to the omission of the quiet sun region. After this point the slope pretty much remains the same.

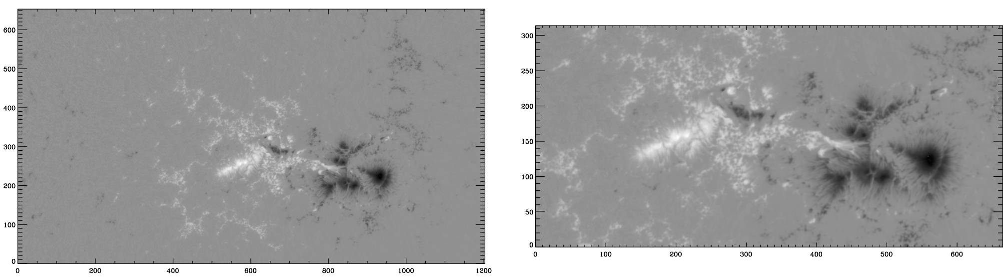

Figure 3.3: Left: Original uncropped image of HARP 1028. Right: Cropped image of HARP 1028.)

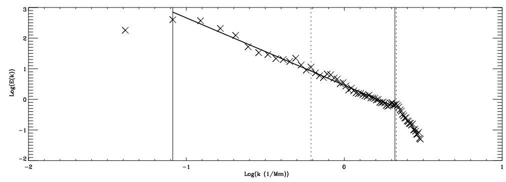


Figure 3.4: Power Spectrum for an MDI/SOHO image of NOAA 10488 taken on 1st Nov. 2003. Dotted vertical lines show the conventional inertial range (3-10 Mm).Solid vertical lines show the inertial range based on spectral discontinuities.

In power index studies, generally, an inertial range is considered to be 3-10 Mm. Figure 3.4 shows a magnetic spectrum for an MDI/SOHO image of an active region NOAA 10488 taken on 1st Nov. 2003. In this diagram we see that the lower limit for the inertial range extends much farther away from wavenumber $2\pi/10$, towards low wave number. $2\pi/3$ is also not a special limit of an inertial range since it depends on the resolution of an image. [2] HMI/SDO magnetograms have better image resolution than MDI/SOHO. In figure (3.1) we can see that the upper limit on the inertial range occurs at a wave number higher than $2\pi/3$.

In our studies inertial range is considered to be a part of the spectrum between two spectral discontinuities, considering all the points within this range for the accurate slope calculation. We observed that in most of the cases, approximately first 65% of the spectrum falls into the inertial range. Hence this criteria is used to obtain the inertial range for all the images.

# Chapter 4

# Results

Power index was computed for HMI active regions as they travelled across the disk. Hence power index evolution can be studied by plotting power index values against time (Fig. 4.1).

## 4.1 Flare Index

SXR flare index was first introduced by [3], by waighing the SXR flares of classes B, C, M and X as 0.1, 1, 10, and 100 respectively. This index gives a measure to flare productivity of a given active region. Clearly, higher flare index indicates higher flare productivity of that region.

Daily SXR flare index can be calculated as [2] :

$$A = (100S^{(X)} + 10S^{(M)} + 1.0S^{(C)} + 0.1S^{(B)})/\tau$$

Here S is the sum of GOES peak intensities of a particular class. (i.e. X, M, C, B classes and intensities are denoted by indices from 1.0 to 9.9 following these classes). and $\tau$ is the time measured in days.

Flare index was calculated for 28 flare-productive regions on a daily basis. Since the power index doesn't change much in a day, flare index value per day was associated with 6-7 power index values per day for all HARPs. Figure 4.2 shows Flare index vs power index graph. In this graph, we can see that the flare index starts increasing as the power index increases, and is maximum around 2.2

## 4.2 Power Index

Figure 4.3 shows an overplot of histograms of all the power index values for all 52 regions. dotted line shows the histogram for non-flaring regions,

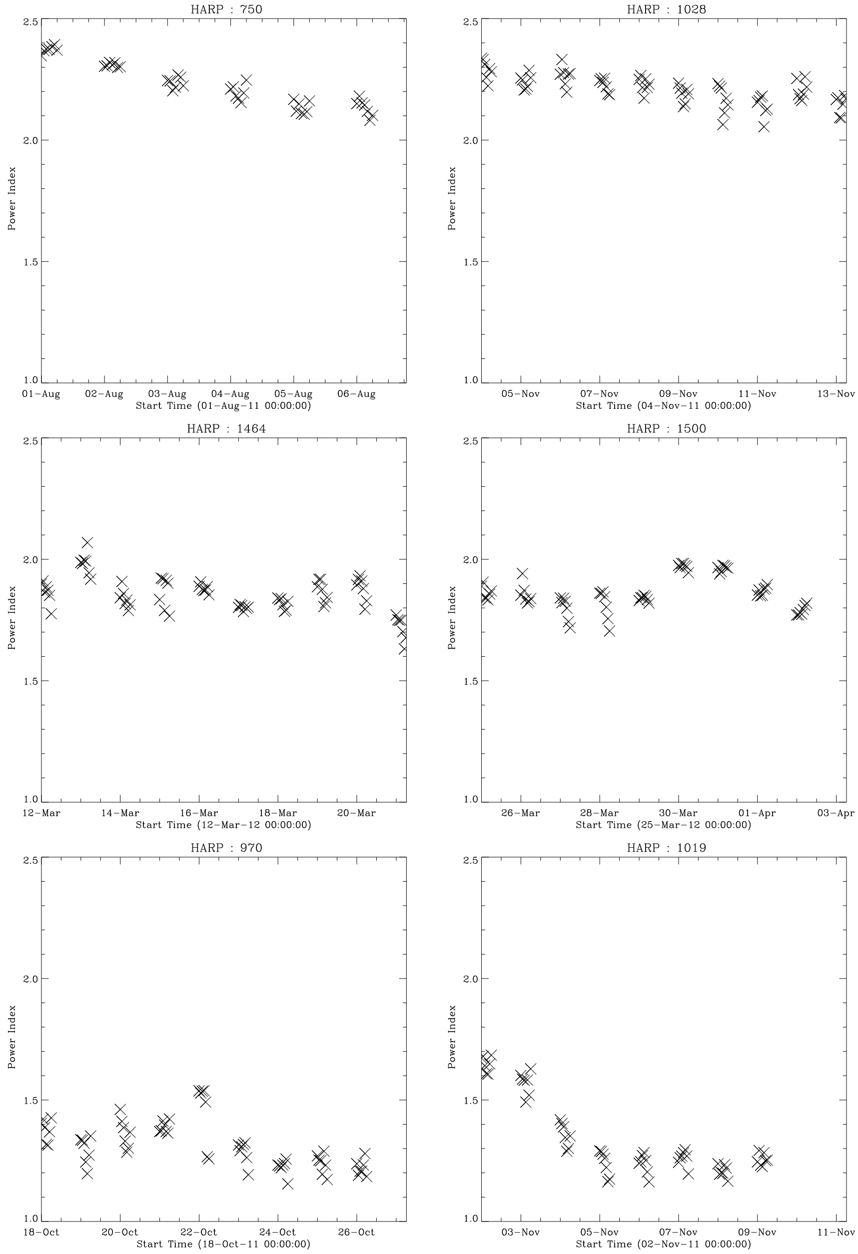


Figure 4.1: First row: Power index evolution for HARP 750 and HARP 1028 that showed high flare activity. Second row: Power index evolution for HARP 1464 and HARP 1500 tat were moderately flare active. Third row: Power index evolution for HARP 970 and HARP 1019 that showed no flare activity.

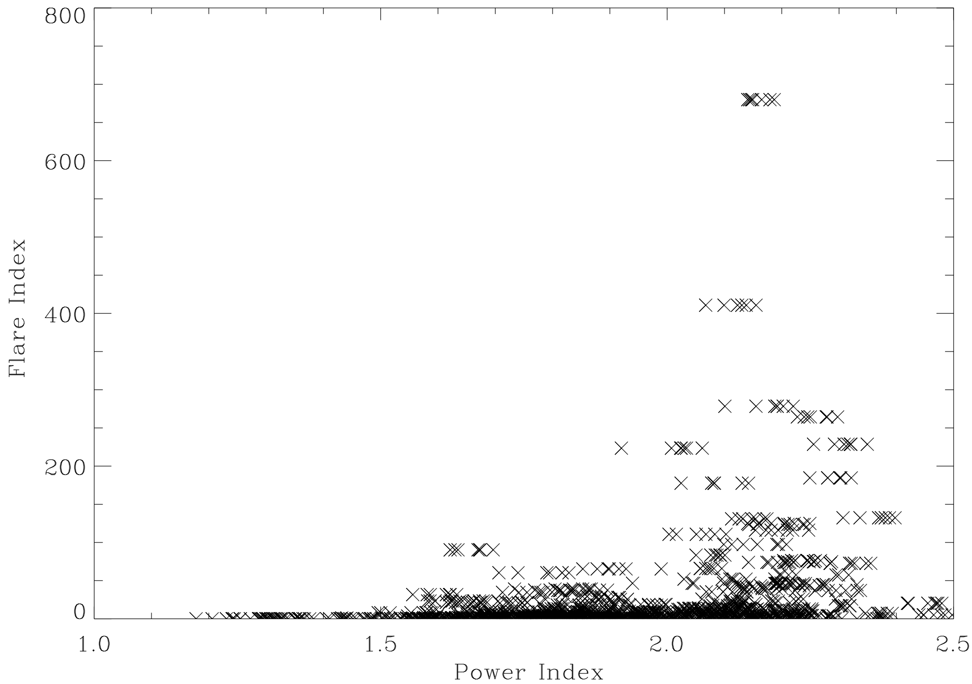


Figure 4.2: Flare index vs Power index graph for 28 Harps that showed flare activity. Flare index increases with increasing power index peaking at 2.2.

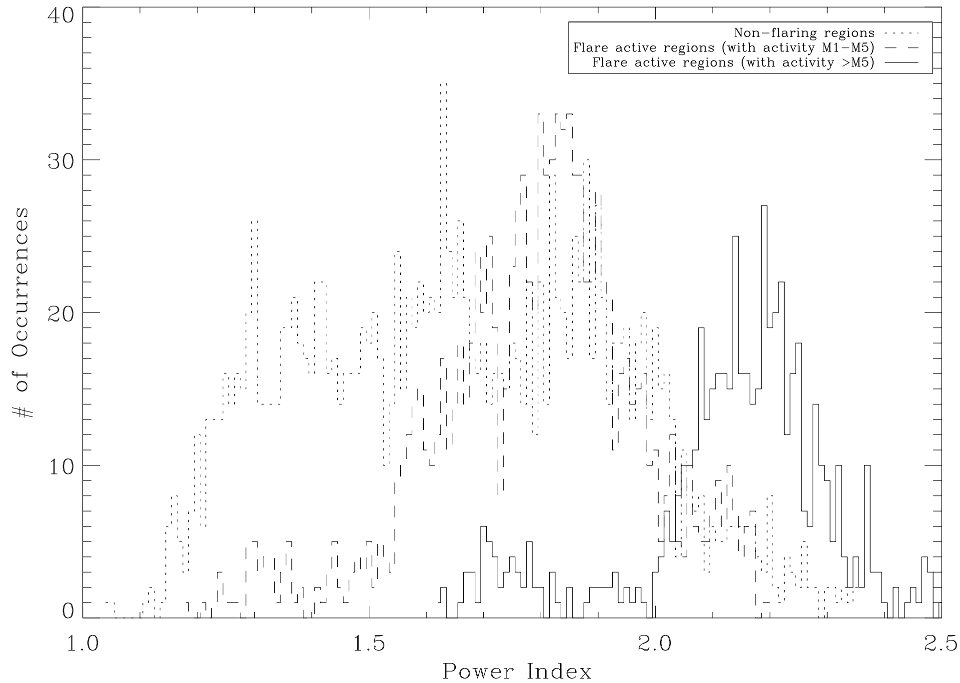


Figure 4.3: Histograms of power index values for all 52 HARPs. Dotted line indicates a histogram for 24 non-flaring regions peaking at 1.6, dashed line shows histogram for 19 HARPs with moderate flare activity peaking at 1.8, whereas solid lines shows histogram for 9 HARPs with high flare activity with peak at 2.2.

dashed line indicates the histogram of regions that gave at least one flare of the intensity between M1 to M5 whereas solid line shows the histogram of highly flare productive regions with at least one flare of the intensity greater than M5. We see that the plots are well separated from each other with maximum for non-flaring occurring at 1.6, maximum for moderately active regions at 1.8 and the maximum for highly flare active regions at 2.2 We also see that, though the graphs are well separated, power index values for non-flaring regions are distributed all over, indicating that high power index is necessary but not a sufficient condition for flaring.

# Chapter 5

# Discussion

Magnetic power spectral analysis was done on 52 HARPs (HMI Active Region Patch) as they travelled across the solar disk. We used Fourier transform to compute power spectrum and power index calculations. Out of which 24 regions showed no flare activity, 19 regions were moderately flare active whereas 9 regions showed high flare activity.

From this study, we reach to the following conclusions:

- In order to calculate power index value for an active region accurately, we need to exclude the quiet sun portion carefully.
- More linear range can be chosen to compute the power index.
- Flare index increases with increase in power index. Flare index value is maximum at around 2.2. Regions with high flare activity likely to have high power index values, around 2.2. Regions with moderate flare activity tend to have power index values around 1.8. Whereas regions that show no flare activity are likely to have power index of 1.6, but may take higher power index values.

Our results indicate that regions that show no flare activity are likely to have Kolmogorov type power spectra ($\sim 5/3$). Kolmogorov type spectra shows the presence of homogeneous stationary turbulence. Regions that showed high flare activity have steeper non-Kolmogorov type spectra. This shows the presence of inhomogeneous non-stationary turbulence.

Though flare quiet regions and highly flare active regions are likely to have Kolmogorov type and steeper, non-Kolmogorov type spectra respectively, flare-quiet regions may also take higher power index values. This shows that high power index value is a necessary but a not a sufficient condition for flaring.

# References

[1] [Abramenko, Yuchyshyn, Wang, and Goode2001] Abramenko, V., Yurchyshyn, V., Wang, H., Goode, P.R.: 2001, **201**, 225.

[2] [Abramenko2005] Abramenko, V.: 2005, ApJ **629**, 1141.

[3] [Antalova1996] Antalova, A.: 1996, Contributions of the Astronomical Observatory Skalnate Pleso **26**, 98.

[4] [Iroshnikov1963] Iroshnikov, P.S.: 1963, Astron.Zh. **40**, 742.

[5] [Kolmogorov1941] Kolmogorov, A.N.: 1941, Acad.Sci.U.S.S.R. **30**, 301.

[6] [Kraichnan1965] Kraichnan, R.H.: 1965, Phys.Fluids **8**, 1385.

[7] [Monin and Yaglom1975] Monin, A.S., Yaglom, A.M.: 1975, in J.Lumley(ed.),Statistical Fluid Mechanics, Vol.2, MIT Press,Cambridge,MA.